Dimensionality of superconductivity in the layered organic material EtMe₃P[Pd(dmit)₂]₂ under pressure

R. Yamamoto,[*] Y. Yanagita, T. Namaizawa, S. Komuro, T. Furukawa, and T. Itou[†]

Department of Applied Physics, Tokyo University of Science, Tokyo 125-8585, Japan

R. Kato

Condensed Molecular Materials Laboratory, RIKEN, Saitama 351-0198, Japan

We measured the ac magnetic susceptibility for the layered organic superconductor EtMe₃P[Pd(dmit)₂]₂ under pressure with a dc magnetic field applied perpendicular to the ac field. We investigated the dc field dependence of the ac susceptibility in detail and concluded that the superconductivity in EtMe₃P[Pd(dmit)₂]₂ is an anisotropic three-dimensional superconductivity even at low temperatures, which contrasts with the large majority of other correlated electron layered superconductors such as high-T_c cuprate and κ-(ET)₂X systems.

I. INTRODUCTION

Layered organic superconductors, as well as layered cuprate superconductors, have been intensively studied in the field of physics of quasi-two-dimensional correlated electron superconductivity. These layered superconductors are classified into two categories according to the ratio of the interlayer coherence length $\xi_\perp$ to the layer distance d. If d is sufficiently shorter than $\xi_\perp$ ($\xi_\perp \gg d$), the system is regarded as an "anisotropic three-dimensional superconductor (A3DSC)," which can be described by the anisotropic Ginzburg-Landau (GL) model [1]. If d is sufficiently longer than $\xi_\perp$ ($\xi_\perp \ll d$), the system is regarded as a "two-dimensional superconductor (2DSC)," that is, a set of weakly coupled discrete two-dimensional superconducting layers. A description of the 2DSC requires the Lawrence-Doniach (LD) model [2], in which the discrete layers are weakly coupled through Josephson terms.

In general, all layered superconductors are A3DSC around the transition temperature T_c under zero magnetic field because $\xi_\perp$ diverges at the transition temperature. Since $\xi_\perp$ decreases on cooling, they can undergo a dimensional crossover to 2DSC at temperature T^*, where $\xi_\perp$ becomes roughly shorter than d. (To be exact, T^* is defined as the temperature where $\xi_\perp$ reaches $d/\sqrt{2}$ [3,4].) Most of the cuprate superconductors and the representative organic superconductors κ-(ET)₂X, where ET denotes bis(ethylenedithio)-tetrathiafulvalene and X is a monovalent anion, undergo the dimensional crossover and show 2DSC natures at low temperatures. For example, the crossover temperature in Bi₂Sr₂CaCu₂O₈₊ₓ is estimated to be $0.99T_c - 0.999T_c$ [1,4–6]. In YBa₂Cu₃O₇₋δ, which has stronger three dimensionality than Bi₂Sr₂CaCu₂O₈₊ₓ, the crossover temperature is estimated to be $0.8T_c - 0.9T_c$ [1,4,7,8].

Recently, a layered organic superconductor, EtMe₃P[Pd(dmit)₂]₂, where Et = C₂H₅, Me = CH₃, and dmit = 1,3-dithiol-2-thione-4,5-dithiolate, C₃S₅, (space group $P2_1/m$) has attracted much attention. It has a nearly isotropic triangular lattice [9,10] and shows a spin-gapped Mott insulating state at ambient pressure [10,11]. When this system is pressurized, superconductivity with $T_c \approx 5$ K appears [9,11–14]. Also note that a very recent work, which discussed the anisotropy of the resistivity, proposed a strong three-dimensional nature in the normal phase of this material [15].

Correlated-electron superconductivities on triangular lattices have attracted much theoretical attention. From an experimental point of view, however, real materials are very limited. One of the few examples is the water-intercalated sodium cobaltate superconductor [16], which was studied very intensively. The experimental results on the superconductivity, however, remain inconclusive [17–21] because the cobaltate superconductor is strongly unstable concerning its chemical, structural, and thus superconducting properties [22,23]. Under such circumstances, EtMe₃P[Pd(dmit)₂]₂ occupies an important position because it shows a stable superconducting state realized in correlated electrons on a triangular lattice. Indeed, the superconductivity of this material looks peculiar because it is adjacent to the spin-gapped phase, which contrasts with most of the other correlated electron superconductors in which the superconducting phase borders a magnetically ordered phase. Thus, the properties of superconductivity in EtMe₃P[Pd(dmit)₂]₂ are intriguing and need to be elucidated. In this study, we report the dimensionality of superconductivity in EtMe₃P[Pd(dmit)₂]₂.

II. EXPERIMENT

We measured the ac susceptibility under pressure for single crystals with a dc magnetic field H_{dc} applied perpendicular to the ac field H_{ac}.

For this purpose, we prepared fine single crystals of EtMe₃P[Pd(dmit)₂]₂ by an aerial oxidation method. The crystals are platelike with a typical area of ∼1 mm² (in the
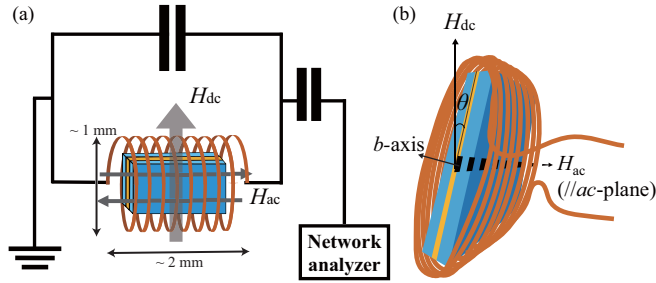
---
[*]1518702@ed.tus.ac.jp
[†]tetsuaki.itou@rs.tus.ac.jp

FIG. 1. (a) LC tank circuit to measure ac susceptibility. dc magnetic field H_{dc} was also applied perpendicular to the ac field H_{ac}. (b) Schematic for the configuration of H_{ac} and H_{dc}. The angle between the directions of the two-dimensional layers and H_{dc} is defined as θ, which was varied by a rotation mechanism.

conducting ac plane) and a typical thickness of $\sim 50\,\mu$m (along the b axis). We inserted a single crystal into a coil, which typically has 125 turns and a dimension $\sim 1 \times 0.5 \times 2$ mm. We packed the arrangement into a Teflon capsule filled with a pressure medium (Daphne 7373 oil). We applied a pressure of ~ 5.0 kbar at room temperature with a BeCu clamp cell. The pressure was estimated from the external force applied at room temperature. Here we emphasize that at low temperatures, the pressure decreases by 1.5–2 kbar from that at room temperature [24]; thus, the actual pressure at low temperatures is 3.0–3.5 kbar. The ac susceptibility measurements were performed for three single crystals and the results showed good reproducibility for all the three crystals.

To estimate the ac susceptibility, we measured the resonance frequency f of the LC tank circuit shown in Fig. 1(a) using a network analyzer (Agilent Technologies E5061A). The ac field H_{ac}, which was produced by the ac electric current generated by the network analyzer and flowing through the coil, was applied nearly parallel to the conducting ac layers. Because the samples are very thin (a typical area of ~ 1 mm^2 and a typical thickness of $\sim 50\,\mu$m), the demagnetization factors for H_{ac} are less than 0.1 and thus ignorable. The magnitude of H_{ac} was about 0.8 Gauss, which is much smaller than the parallel lower-critical field $H_{c1}^{\parallel}$ at low temperatures [14]. Since f is proportional to the inverse of the square root of the coil inductance L ($f = 1/2\pi\sqrt{LC} = f_0/\sqrt{1+4\pi\eta\chi}$), the relation between f and the ac susceptibility χ is denoted by

$$-4\pi\chi = \frac{1}{\eta}\left(1 - \frac{f_0^2}{f^2}\right), \quad (1)$$

where f_0 is the resonance frequency of the tank circuit when the sample is in the normal state, and η is the filling factor that reflects the ratio of the sample volume to the coil volume. In the three measurements made for the three samples, the values of η are 0.027, 0.033, 0.13 and have uncertainties of $\pm 50\%$.

In addition to H_{ac}, H_{dc} was applied perpendicular to H_{ac} by a superconducting magnet. The angle between the directions of the two-dimensional layers of EtMe$_3$P[Pd(dmit)$_2$]$_2$ and H_{dc} is defined as θ, as shown in Fig. 1(b); $\theta = 0°$ shows that H_{dc} is exactly parallel to the two-dimensional layers. The angle θ was rotated within $\theta = \pm 15°$ with a rotation pitch of 0.18°.
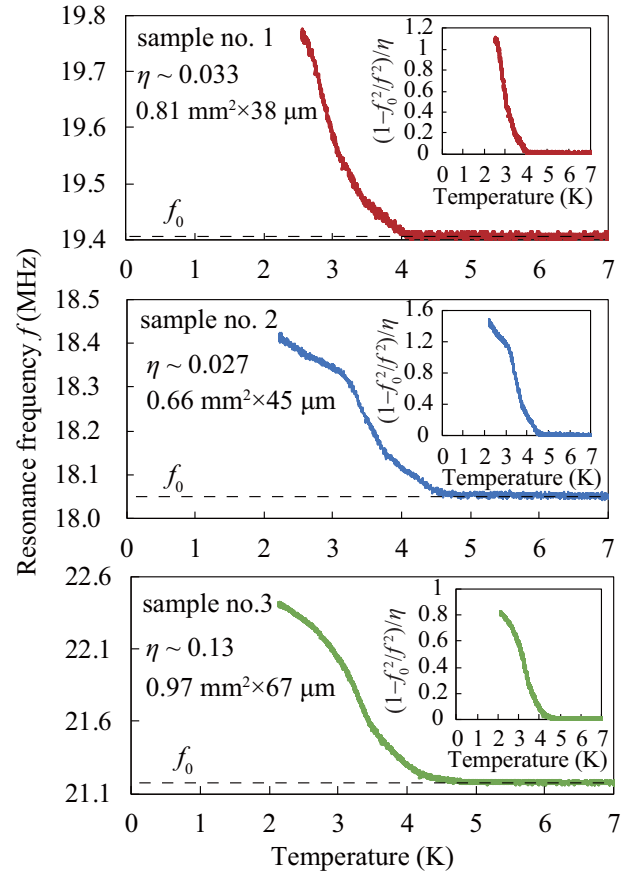

FIG. 2. Temperature dependence of the resonance frequency f of the LC tank circuit under $H_{dc} = 0$ T. The insets show the temperature dependence of $1/\eta(1 - f_0^2/f^2)$, where η is ~ 0.033 for sample no. 1, ~ 0.027 for sample no. 2, and ~ 0.13 for sample no. 3. Note that the values of η have uncertainties of $\pm 50\%$. It is also noted that the sample thickness is $\sim 50\,\mu$m and thus the magnetic penetration effect is not ignorable.

III. RESULTS AND DISCUSSION

A. Diamagnetic signal under $H_{dc} = 0$ T

Figure 2 shows the temperature dependence of f under $H_{dc} = 0$ T. As shown in this figure, the diamagnetic susceptibility due to the Meissner effect is observed as an increase in f. The insets show the temperature dependence of $1/\eta(1 - f_0^2/f^2)$, which, as per Eq. (1), gives $-4\pi\chi$. We note again that η has uncertainties of $\pm 50\%$.

The volume fraction of the superconductivity, which is estimated from the magnitude of $-4\pi\chi$, is of the order of 100% for all the samples at the lowest measured temperature, 2.2 K. Although η has considerable uncertainty, this result confirms that the present superconductivity is bulk, which is consistent with the results of the previously reported susceptibility measurements obtained using a superconducting quantum interference device (SQUID) magnetometer [14].

As shown in the insets of Fig. 2, the diamagnetic signal increases rather gradually. An obvious reason for this gradual increase is the magnetic penetration effect. Around T_c, the penetration length λ tends to diverge and becomes comparable to or longer than the sample thickness of $\sim 50\,\mu$m, which
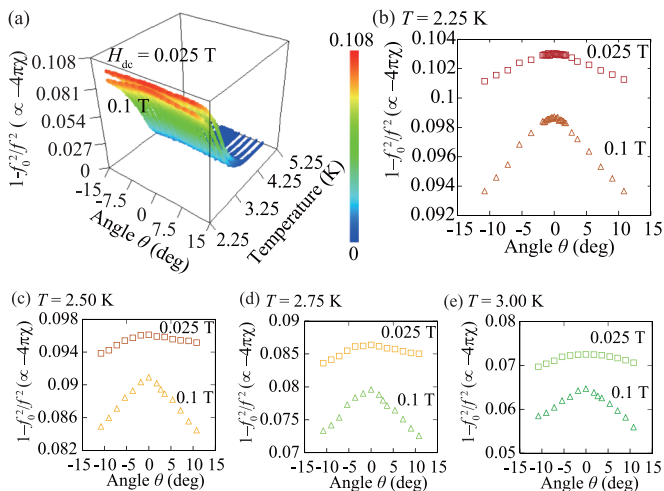
FIG. 3. (a) Temperature dependence of $1 - f_0^2/f^2$ at various angles θ under $H_{dc} = 0.025$ and 0.1 T. (b–e) Angle dependence of $1 - f_0^2/f^2$ under $H_{dc} = 0.025$ (squares) and 0.1 T (triangles), derived from the data in Fig. 3(a).

FIG. 4. (a) Temperature dependence of $1 - f_0^2/f^2$ at various H_{dc} at $\theta = 0°$. (b) Temperature dependence of $H_{c2}^{\parallel}$ indicated by the arrows in Fig. 4(a).

suppresses the diamagnetic signal. Another possible reason is that the transition temperature T_c may be distributed to some degree due to possible pressure inhomogeneity or crystal imperfections.

B. Angle dependence of the diamagnetic signal

In contrast to A3DSC, 2DSC generally exhibits the lock-in state with Josephson vortices trapped in insulating layers when H_{dc} is applied nearly parallel to the two-dimensional layers [25]. In other words, whether the lock-in state is realized or not provides strong information about the dimensionality of superconductivity.

When the lock-in state is realized, the ac diamagnetic signal (response to H_{ac} parallel to the two-dimensional layers and perpendicular to H_{dc}) is strongly suppressed because the vortices can easily tilt according to the applied H_{ac} [25]. Therefore, the ac diamagnetic signal has a characteristic dependence on the angle between the directions of the two-dimensional layers and H_{dc}, showing a strong depression where they are parallel to each other.

As explained in the Experiment section, we performed ac susceptibility measurements with H_{dc} applied perpendicular to the ac field H_{ac}. The three samples that we measured show reproducible results, and hereinafter we show data obtained for sample no. 3.

Figure 3(a) shows the temperature dependence of $1 - f_0^2/f^2$ at various values of θ under $H_{dc} = 0.025$ and 0.10 T. Figure 3(b) shows the angle θ dependence of $1 - f_0^2/f^2$ ($\propto -4\pi\chi$) at 2.25 K, derived from the data in Fig. 3(a). The angle dependence shows no depression around $\theta = 0°$, which indicates that the lock-in state is not observed in this experimental condition. For the representative organic two-dimensional superconductor κ-(ET)$_2$Cu(NCS)$_2$, the lock-in angle is reported to be within $\pm 10°$ under 0.1 T and within $\pm 30°$ under 0.02 T [25]. Indeed, the lock-in angle in the present material for $H_{dc} = 0.1$ and 0.025 T is roughly estimated to be within $\pm 1.7°$ and $\pm 7.0°$, respectively, by assuming the rough
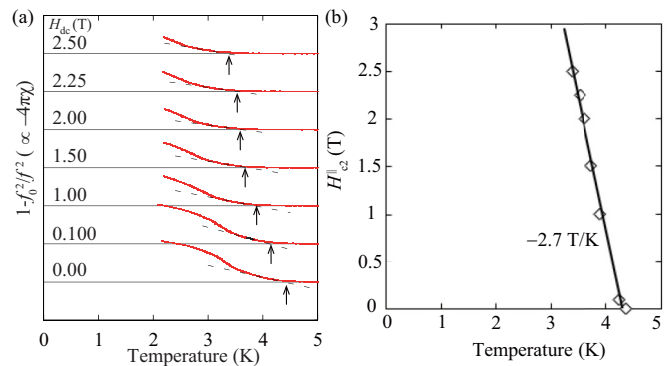
lock-in condition $H_{dc} \sin\theta < H_{c1}^{\perp}$, and the reported value of $H_{c1}^{\perp} = 0.003$ T [14]. This estimation is very naive, and the true values of the lock-in angle may be smaller than the estimated values. However, the estimated values (in particular, for $H_{dc} = 0.025$ T) are much larger than the present experimental rotation pitch of $0.18°$. Thus, the angle resolution is sufficient to detect the lock-in state if it exists. Therefore, we can definitely say that the superconductivity in EtMe$_3$P[Pd(dmit)$_2$]$_2$ never realizes the lock-in state at 2.25 K. This clearly suggests that the present superconductivity is an A3DSC even at temperatures much lower than T_c (even at 0.5 T_c).

C. H–T phase diagram

When dc field is applied parallel to the two-dimensional layers of a layered superconductor, the upper critical field just below T_c is written as

$$H_{c2}^{\parallel}(T) = \frac{\phi_0}{2\pi\xi_{\parallel}(T)\xi_{\perp}(T)}, \qquad (2)$$

where ϕ_0 is the flux quantum, and $\xi_{\parallel}$ ($\xi_{\perp}$) is the intralayer (interlayer) coherence length. Thus, the data on $H_{c2}^{\parallel}$ gives information on the coherence lengths, giving additional supportive insight into the dimensionality of the superconductivity.

As explained in the Experiment section, we performed ac susceptibility measurements under H_{dc}. We fixed the direction of H_{dc} to be $\theta = 0°$ and obtained $1 - f_0^2/f^2$ under several H_{dc} values, as shown in Fig. 4(a). Figure 4(b) shows the temperature dependence of $H_{c2}^{\parallel}$, indicated by the arrows in Fig. 4(a). The initial value of the gradient ($dH_{c2}^{\parallel}/dT$ around T_c) is -2.7 T/K. This value is less than half of the value in κ-(ET)$_2$Cu$_2$(CN)$_3$ (-6.6 T/K) [26]. Note that κ-(ET)$_2$Cu$_2$(CN)$_3$ is also the nearly isotropic triangular lattice system with almost the same transfer integrals [27–29] and electron correlation energies [28,29] as those in EtMe$_3$P[Pd(dmit)$_2$]$_2$ and has T_c ($=3.8$ K [30,31]) near that in EtMe$_3$P[Pd(dmit)$_2$]$_2$. Since the intralayer coherence length $\xi_{\parallel}$ is generally dominated by the main energy scales of superconductivity, it is natural to think that $\xi_{\parallel}$ is almost the same in κ-(ET)$_2$Cu$_2$(CN)$_3$ and EtMe$_3$P[Pd(dmit)$_2$]$_2$. Consequently, the small value of $dH_{c2}^{\parallel}/dT$ around T_c in EtMe$_3$P[Pd(dmit)$_2$]$_2$ very likely indicates that $\xi_{\perp}$ in EtMe$_3$P[Pd(dmit)$_2$]$_2$ is much longer than

$\xi_\perp$ in κ-(ET)$_2$Cu$_2$(CN)$_3$. This is consistent with the previously discussed conclusion that the superconductivity in EtMe$_3$P[Pd(dmit)$_2$]$_2$ is an A3DSC.

D. Angle dependence of the transition temperature

The angle θ dependences of the upper critical field $H_{c2}(\theta)$ for 2DSC and A3DSC are distinguishable; thus, $H_{c2}(\theta)$ gives supporting information on the dimensionality of superconductivity.

For 2DSC, the Tinkham model gives the following relation of $H_{c2}(\theta)$ [1,32]:

$$\left| \frac{H_{c2}(\theta)\sin\theta}{H_{c2}^\perp} \right| + \left(\frac{H_{c2}(\theta)\cos\theta}{H_{c2}^\parallel} \right)^2 = 1, \qquad (3)$$

where $H_{c2}^\perp$ ($H_{c2}^\parallel$) is the upper critical field when the dc field is applied perpendicular (parallel) to the two-dimensional layers. Note that the angle dependence of $H_{c2}(\theta)$ derived from Eq. (3) shows a cusp at $\theta = 0°$.

For A3DSC, according to the anisotropic GL model, $H_{c2}(\theta)$ satisfies the following relation [1,2]:

$$\left(\frac{H_{c2}(\theta)\sin\theta}{H_{c2}^\perp} \right)^2 + \left(\frac{H_{c2}(\theta)\cos\theta}{H_{c2}^\parallel} \right)^2 = 1. \qquad (4)$$

In contrast to 2DSC, the angle dependence of $H_{c2}(\theta)$ derived from Eq. (4) shows a smooth behavior at $\theta = 0°$ without a cusp.

The singularity in the angle dependence of the transition temperature T_c is essentially the same as that in $H_{c2}(\theta)$ because $\frac{\partial T_c(H,\theta)}{\partial\theta} = \frac{\partial T_c(H,\theta)}{\partial H}\left(\frac{dH_{c2}(\theta)}{d\theta}\right)_{T=T_c}$ and $\frac{\partial T_c(H,\theta)}{\partial H} \neq 0$. Accordingly, the angle dependence of T_c shows a cusp at $\theta = 0°$ in 2DSC and no cusp in A3DSC.

Indeed, according to Welp *et al.* [7], T_c for 2DSC and A3DSC satisfies the following relations, which shows a cusp and a smooth behavior, respectively.

For 2DSC,

$$T_c(H,\theta) = T_{c0} - |(T_{c0} - T_c^\perp(H))\sin\theta| \\ - (T_{c0} - T_c^\parallel(H))\cos^2\theta, \qquad (5)$$

where T_{c0} is the transition temperature at $H = 0$, and $T_c^\perp(H)$ and $T_c^\parallel(H)$ are the transition temperature when H is applied perpendicular and parallel to the conducting layers, respectively.

For A3DSC,

$$T_c(H,\theta) = T_{c0} + \frac{H}{dH_{c2}^\parallel(T)/dT}\left(\cos^2\theta + \frac{m^\perp}{m^\parallel}\sin^2\theta \right)^{1/2}, \qquad (6)$$

where $m^\perp/m^\parallel$ is the anisotropic factor of the A3DSC.

Figure 5(a) shows the temperature dependence of $1 - f_0^2/f^2$ at various angles θ under $H_{dc} = 1$ T. Figure 5(b) shows the angle dependence of T_c, which is defined as the temperature where the ac diamagnetic signal starts to appear, shown in the arrows in Fig. 5(a). As seen in this figure, the angle dependence of T_c (which is approximately 3.9 K at $\theta = 0°$) does not show a cusp but shows smooth behavior at $\theta = 0°$.
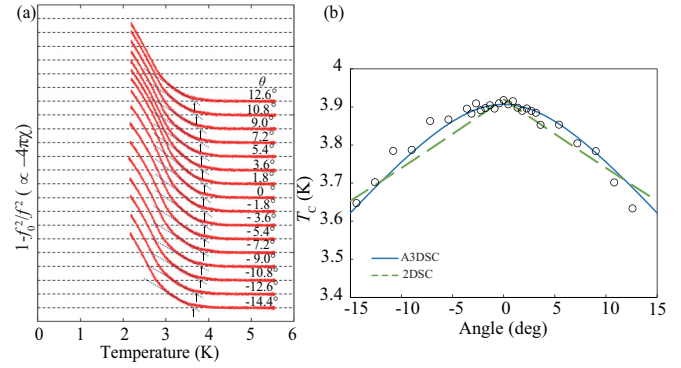

FIG. 5. (a) Temperature dependence of $1 - f_0^2/f^2$ at various angles θ under $H_{dc} = 1$ T. (b) Angle dependence of the transition temperature T_c, indicated by the arrows in Fig. 5(a). The solid and dashed lines are the fitted curves of the A3DSC and 2DSC models, respectively. The A3DSC model can fit the data very well, while the 2DSC model cannot.

Furthermore, it is well fitted by the A3DSC model [Eq. (6)] while it is not fitted by the 2DSC model [Eq. (5)]. In this A3DSC model fitting, T_{c0} and $m^\perp/m^\parallel$ are treated as fitting parameters and $dH_{c2}^\parallel(T)/dT$ is set to be a constant value -2.7 T/K, which is obtained by the data shown in Fig. 4(b). The best fitting shown in the solid line in Fig. 5(b) gives $m^\perp/m^\parallel = 32 \pm 6$.

In order to check the reliability of this fitting by the A3DSC model, we also performed preliminary $H_{c2}^\perp$ measurement under the condition that the dc magnetic field is applied perpendicular to the conducting layers. Although this measurement was done for one sample and in this sense is preliminary, the observed value of $dH_{c2}^\perp(T)/dT$ just below the transition temperature is about one-sixth of that of $dH_{c2}^\parallel(T)/dT$, which is shown in Fig. 4(b). Because this ratio is proportional to the inverse of the square of the anisotropic factor $m^\perp/m^\parallel$, this result indicates that $m^\perp/m^\parallel$ is approximately $6^2 = 36$. This is well consistent with the above estimated value 32 ± 6 obtained by the A3DSC model fitting, giving further evidence that the present superconductivity is explained by the A3DSC model. This result gives additional supportive evidence for the conclusion that the superconductivity in EtMe$_3$P[Pd(dmit)$_2$]$_2$ is an A3DSC (at least at the temperature around 3.9 K).

E. The molecular orbital

As discussed previously, we concluded that the superconductivity in EtMe$_3$P[Pd(dmit)$_2$]$_2$ under pressure is an A3DSC even at low temperatures, which is in striking contrast to the large majority of other correlated electron layered superconductors such as cuprate and κ-(ET)$_2X$ systems. In this section, we discuss the reasons for the realization of this peculiar superconductivity in EtMe$_3$P[Pd(dmit)$_2$]$_2$.

In the ET molecule, the terminal hydrogen atoms negligibly contribute to the molecular orbital that forms the conduction band [33]. This explains the weak interlayer coupling in the κ-(ET)$_2X$ system because the interlayer coupling is caused by the orbital overlap between the terminal atoms in these organic systems. In contrast, the terminal atoms of the Pd(dmit)$_2$ molecule are sulfur, and the molecular orbital

density of $Pd(dmit)_2$ at Fermi energy is spread to these sulfur atoms [34,35]. In addition, the smallest interlayer S–S distance in $EtMe_3P[Pd(dmit)_2]_2$ is especially short (3.6753 Å) among the $X[Pd(dmit)_2]_2$ system. Hence the strong interlayer coupling is expected in $EtMe_3P[Pd(dmit)_2]_2$. This is the probable cause of the present peculiarity of the superconductivity in $EtMe_3P[Pd(dmit)_2]_2$.

IV. CONCLUSION

We have investigated the dimensionality of superconductivity in $EtMe_3P[Pd(dmit)_2]_2$ under pressure by ac susceptibility measurements with the application of dc magnetic field. We have obtained the following three results: (i) The angle θ dependence of the ac susceptibility at 2.25 K shows no depression around $\theta = 0°$. This clearly indicates that the lock-in state, which is characteristic of 2DSC, is not realized in the present system. (ii) The angle dependence of T_c does not show a cusp but shows smooth behavior at $\theta = 0°$. (iii) The value of $H_{c2}^{\parallel}$ just below T_c in $EtMe_3P[Pd(dmit)_2]_2$ is much smaller than that in $\kappa\text{-}(ET)_2Cu_2(CN)_3$. This indicates that the interlayer coherence length $\xi_\perp$ in $EtMe_3P[Pd(dmit)_2]_2$ is much longer than that in $\kappa\text{-}(ET)_2X$. From these results, we conclude that the superconductivity in $EtMe_3P[Pd(dmit)_2]_2$ is an A3DSC even at temperatures much lower than T_c (even at $\sim 0.5\,T_c$).

[1] M. Tinkham, *Introduction to Superconductivity*, 2nd ed. (Dover, New York, 2004).

[2] W. E. Lawrence and S. Doniach, in *Proceedings of the 12th International Conference on Low Temperature Physics*, edited by E. Kanda (Keikagu, Tokyo, 1971).

[3] R. A. Klemm, A. Luther, and M. R. Beasley, Phys. Rev. B **12**, 877 (1975).

[4] T. Schneider and A. Schmidt, Phys. Rev. B **47**, 5915 (1993).

[5] R. Marcon, E. Silva, R. Fastampa, and M. Giura, Phys. Rev. B **46**, 3612 (1992).

[6] J. R. Clem, M. W. Coffey, and Z. Hao, Phys. Rev. B **44**, 2732 (1991).

[7] U. Welp, W. K. Kwok, G. W. Crabtree, K. G. Vandervoort, and J. Z. Liu, Phys. Rev. B **40**, 5263 (1989).

[8] D. E. Farrell, J. P. Rice, D. M. Ginsberg, and J. Z. Liu, Phys. Rev. Lett. **64**, 1573 (1990).

[9] R. Kato, A. Tajima, A. Nakao, and M. Tamura, J. Am. Chem. Soc. **128**, 10016 (2006).

[10] M. Tamura, A. Nakao, and R. Kato, J. Phys. Soc. Jpn. **75**, 093701 (2006).

[11] T. Itou, A. Oyamada, S. Maegawa, K. Kubo, H. M. Yamamoto, and R. Kato, Phys. Rev. B **79**, 174517 (2009).

[12] M. Tamura, Y. Ishii, and R. Kato, J. Phys.: Condens. Matter **19**, 145239 (2007).

[13] Y. Shimizu, H. Akimoto, H. Tsujii, A. Tajima, and R. Kato, Phys. Rev. Lett. **99**, 256403 (2007).

[14] Y. Ishii, M. Tamura, and R. Kato, J. Phys. Soc. Jpn. **76**, 033704 (2007).

[15] Y. Shimizu and R. Kato, Phys. Rev. B **97**, 125107 (2018).

[16] K. Takada, H. Sakurai, E. Takayama-Muromachi, F. Izumi, R. A. Dilanian, and T. Sasaki, Nature (London) **422**, 53 (2003).

[17] T. Fujimoto, G. Q. Zheng, Y. Kitaoka, R. L. Meng, J. Cmaidalka, and C. W. Chu, Phys. Rev. Lett. **92**, 047004 (2004).

[18] M. M. Maśka, M. Mierzejewski, B. Andrzejewski, M. L. Foo, R. J. Cava, and T. Klimczuk, Phys. Rev. B **70**, 144516 (2004).

[19] W. Higemoto, K. Ohishi, A. Koda, S. R. Saha, R. Kadono, K. Ishida, K. Takada, H. Sakurai, E. Takayama-Muromachi, and T. Sasaki, Phys. Rev. B **70**, 134508 (2004).

[20] Y. Ihara, K. Ishida, C. Michioka, M. Kato, K. Yoshimura, K. Takada, T. Sasaki, H. Sakurai, and E. Takayama-Muromachi, J. Phys. Soc. Jpn. **73**, 2069 (2004).

[21] M. Kato, C. Michioka, T. Waki, Y. Itoh, K. Yoshimura, K. Ishida, H. Sakurai, E. Takayama-Muromachi, K. Takada, and T. Sasaki, J. Phys.: Condens. Matter **18**, 669 (2006).

[22] M. L. Foo, R. E. Schaak, V. L. Miller, T. Klimczuk, N. S. Rogado, Y. Wang, G. C. Lau, C. Craley, H. W. Zandbergen, N. P. Ong, and R. J. Cava, Solid State Commun. **127**, 33 (2003).

[23] D. P. Chen, H. C. Chen, A. Maljuk, A. Kulakov, H. Zhang, P. Lemmens, and C. T. Lin, Phys. Rev. B **70**, 024506 (2004).

[24] K. Murata, H. Yoshino, H. O. Yadav, Y. Honda, and N. Shirakawa, Rev. Sci. Instrum. **68**, 2490 (1997).

[25] P. A. Mansky, P. M. Chaikin, and R. C. Haddon, Phys. Rev. Lett. **70**, 1323 (1993).

[26] K. Kanoda (private communication).

[27] T. Komatsu, N. Matsukawa, T. Inoue, and G. Saito, J. Phys. Soc. Jpn. **65**, 1340 (1996).

[28] K. Nakamura, Y. Yoshimoto, T. Kosugi, R. Arita, and M. Imada, J. Phys. Soc. Jpn. **78**, 083710 (2009).

[29] K. Nakamura, Y. Yoshimoto, and M. Imada, Phys. Rev. B **86**, 205117 (2012).

[30] Y. Shimizu, H. Kasahara, T. Furuta, K. Miyagawa, K. Kanoda, M. Maesato, and G. Saito, Phys. Rev. B **81**, 224508 (2010).

[31] Y. Kurosaki, Y. Shimizu, K. Miyagawa, K. Kanoda, and G. Saito, Phys. Rev. Lett. **95**, 177001 (2005).

[32] M. Tinkham, Phys. Rev. **129**, 2413 (1963).

[33] E. Scriven and B. J. Powell, Phys. Rev. B **80**, 205107 (2009).

[34] A. E. Underhill, R. A. Clark, I. Marsden, M. Allan, R. H. Friend, H. Tajimas, T. Naito, M. Tamura, H. Kuroda, and A. Kobayashi, J. Phys.: Condens. Matter **3**, 933 (1991).

[35] T. Tsumuraya, H. Seo, M. Tsuchiizu, R. Kato, and T. Miyazaki, J. Phys. Soc. Jpn. **82**, 033709 (2013).